International Journal of Refrigeration 166 (2024) 129–138

Contents lists available at ScienceDirect

International Journal of Refrigeration

journal homepage: www.elsevier.com/locate/ijrefrig

Sorption kinetics of salt-in-porous-matrix composites: The effect of expanded natural graphite on cooling power

Cinétique de sorption des composites sel-matrice poreuse : effet du graphite naturel expansé sur la puissance de refroidissement

Salman Hassanabadi, Ilya S. Girnik, Majid Bahrami *

Laboratory for Alternative Energy Conversion (LAEC), School of Mechatronic Systems Engineering, Simon Fraser University, Surrey, BC, Canada

ARTICLE INFO

Keywords:
Sorption heat transformer
Salt in porous matrix
Expanded natural graphite
Sorption kinetics
Sorption composite

Mots clés:
Transformateurs de chaleur à sorption
Sel dans une matrice poreuse
Graphite naturel expansé
Cinétique de sorption
Composite à sorption

ABSTRACT

Sorption heat transformers and thermal energy storage systems are emerging technologies that utilize and store low-grade waste heat for heating and cooling applications. The performance of sorption systems is not only affected by systems' operating conditions, and overall systems' design but also by sorption material or composite parameters such as thermal diffusivity, composition, and pore structure, among others. In this study, $CaCl_2$-based salt-in-porous-matrix composites of different compositions and coating thicknesses were synthesized. During synthesis, salt to silica gel and polyvinyl alcohol to silica gel ratios were fixed and the thermal additive (expanded natural graphite) to silica gel ratio was varied with care from 0 to 0.26 (or 0 to 20.5 wt.%, additive to silica gel ratio). The thickness of samples varied from 2.3 to 8.3 ± 0.1 mm. The composites were characterized by a transient plane source (thermal conductivity and thermal diffusivity), nitrogen adsorption porosimetry (specific surface area and total pore volume), and thermogravimetric sorption analysis (water sorption equilibrium) methods. A custom-built gravimetric large pressure jump (G-LPJ) testbed was used to study water sorption kinetics (water uptake vs. time) for selected samples. The thermal conductivity and diffusivity of the studied composite samples have shown significant enhancements, e.g., 240% (0.11 W/(m·K) vs. 0.37 W/(m·K)) and 310% (0.21 mm^2/s vs. 0.87 mm^2/s), respectively, by adding 12.5 wt.% expanded natural graphite (additive to silica gel ratio is 0.14) as a thermally conductive additive (additive to silica gel ratio) because of thermal percolation effect. This ratio of expanded natural graphite to silica gel was found to be optimal for studied composition. The results indicate that sorption composites with higher thermal diffusivity offer notably higher specific cooling power and improved sorption kinetics, compared to the composites without expanded natural graphite of the same thickness (850 W/kg vs. 480 W/kg at 70% water conversion for samples with thickness of 5.3 mm).

1. Introduction

As a result of rising extreme climate events, environmental impacts, and increasing energy demand, the need for new methods of heating and cooling using environmentally friendly methods has received immense attention. One such method is sorption heat transformation and thermal energy storage, where a waste-heat-driven sorption process is used for heat pumping, air conditioning and heat and cold storage [1]. The performance of such sorption systems greatly depends on the sorbent material used. Composites synthesized based on inorganic salt-impregnated silica gels, i.e., Salt-in-Porous-Matrix, are of great interest due to their high active surface area, superior sorption kinetics, and high sorption capacity [2,3,4,5,6].

A sorber bed – the reactor containing sorbent material, either as loose grains or as a coating, and a heat exchanger to transfer heat to/from the sorbent material – is the main component of sorption systems and has a significant impact on the system's performance, size, and cost. Therefore, considerable attention has been directed towards developing efficient sorber beds in recent years [7,8,9,10,11,12,13]. However, to achieve optimal system performance, it is also necessary to have an in-depth understanding of the sorbent's characteristics, including

* Corresponding author.
E-mail address: mbahrami@sfu.ca (M. Bahrami).

https://doi.org/10.1016/j.ijrefrig.2024.07.004
Received 29 March 2024; Received in revised form 4 June 2024; Accepted 6 July 2024
Available online 25 July 2024

Nomenclature

m	mass, kg
c_p	specific heat capacity, J/kg K
h	enthalpy, J/kg
k	thermal conductivity, W/m.K
Q	Heat, J
S	surface of the substrate, m^2
SCP	specific cooling power, W/kg
SSCP	SCP multiplied by the mass of the composite (m) and divided by surface of the substrate, W/m^2

Subscripts

evap	evaporation
sorp	sorption
cycle	sorption cycle time

Greek symbols

α	thermal diffusivity, m^2/s
ω	adsorbate uptake, g/g dry sorbent
ρ	density, kg/m^3
τ	Time, s

morphology, chemical composition, and sorption kinetics under selected operating conditions.

Various adsorbent materials can be used as sorbent in sorption systems and a significant amount of research is focused on characterization and evaluating the sorption performance of different materials. Zeolites, as an example, with their porous crystalline structures, exhibit high selectivity and capacity due to their tailored pore sizes and shapes, making them ideal for gas separation and catalysis [14]. Metal-organic frameworks (MOFs) offer remarkable surface areas and tunable pore sizes, enabling precise control over adsorption properties for diverse applications [15]. Silica gels, known for their amorphous structures and abundant surface hydroxyl groups, find extensive use in desiccants due to their high affinity for water molecules [4,9]. Each adsorbent material brings unique characteristics to sorption processes, providing tailored solutions for a wide range of industrial and environmental challenges.

Water vapor and silica gel as a sorptive and sorbent pair in sorption systems received notable attention because of their desirable characteristics including environmental friendliness, non-corrosiveness, non-toxicity, cost-effectiveness, and availability, to name a few [14,16,17]. This working pair is suitable for applications, where low-grade heat sources are available, i.e., temperature less than 100 °C [3].

A disadvantage of micro-/meso-porous silica gels is their low water uptake capacity compared to some other sorbents, such as metal-organic frameworks (MOFs, [18]) and aluminophosphates [19]. One approach to improve their uptake is to use silica gel as a host matrix for hygroscopic salts, such as $CaCl_2$ or LiCl [2]. This modification significantly improves the composite's sorption capacity, while maintaining a relatively low cost for the final material. However, there are several other parameters such as particle size, pore size distribution, specific surface area, and pore geometry which can affect the performance of sorption material and, as a result, of the entire sorption system. These parameters define how well water vapor moves between and inside sorbent grains (vapor diffusivity) during sorption and desorption (i.e. mass transfer) which can affect the rate of both of these processes.

Efficient heat transfer is also important for the sorption process. Because sorption is an exothermal process, for continuous and effective sorption cooling of the sorbent material is required. Since heat generation during sorption is a transient process, the heat transfer within the materials is defined by the thermal diffusivity (Eq. 1):

$$\alpha = \frac{k}{\rho c_p} \tag{1}$$

where, k, ρ, c_p are the thermal conductivity, density, and specific heat capacity of the sorbent material, respectively.

The relatively low thermal conductivity and diffusivity of silica gel (i.e., ~ 0.1–0.2 W/(m·K) and ~ 0.2–0.3 mm^2/s [20,21]) can lead to slow sorption and/or a need for larger heat exchange areas in sorber beds, which will impact the thermal inertia of the bed which consequently lead to lower performance and larger size/cost of the final system. To remedy this issue, researchers have added various thermally conductive additives to the sorbents. Fayazmanesh et al. [22] discovered that by adding natural graphite flakes to a silica gel/polyvinylpyrrolidone (PVP) composite sorbent thermal conductivity increased from about 0.13 W/(m·K) to 0.28 W/(m·K) (115% enhancement) and 0.37 0.13 W/(m·K) (184% enhancement) for 20 wt.% and 40 wt.% of natural graphite flakes, respectively. However, adding more thermally conductive additives to a composite will reduce its active material thus the uptake capacity.

In another study, Bahrehmand et al. [5] did a similar study for silica gel composite containing calcium chloride as hygroscopic salt. They reported up to a 500% enhancement in thermal diffusivity by adding 20 wt.% natural graphite flakes to the composite which leads to the increase of the specific power during sorption by 67%. Authors reported that the increase in the thermal diffusivity of the composite is more pronounced for samples with more than 10 wt.% graphite flakes - "hockey stick" behavior – that can be explained by thermal percolation.

Percolation effect is usually observed for multi-component polymer blends (an electrically conducting filler in an insulating matrix) as a rapid increase of electrical conductivity (e.g. from $\sim 10^{-14}$–10^{-12} to 10^{-3}–10^{-1} S/m) due to the formation of a conductive network by filler material inside the matrix [23]. A similar percolation effect can be observed for the heat conduction process (thermal percolation) in the case of thermally conducting fillers: rapid increase of thermal conductivity and thermal diffusivity when thermally conducting particles produce connected pathways for the heat transfer [23,24]. The thermal percolation effect, though, is less pronounced because usually, thermally conductive additives (fillers) have thermal conductivity only 10–10^3 times higher than that of the matrix, there is a possibility of a bad contact between filler and matrix or due to phonons, which are the main thermal energy carrier, behavior [24].

In the case of both [5] and [22], PVP (matrix) and graphite flakes (filler) produce a thermally conductive mixture which is responsible for the heat transfer from heat-generating sorbent grains to the heat exchanger. However, it is difficult to distinguish the effect of graphite flakes on heat transfer from the effect of binder (PVP). When graphite flakes are added to the sorption material both PVP/silica gel and graphite flakes/silica gel ratios change. Practically this means that when graphite flakes are added to the sorption composite the volume of PVP binder changes per grain of silica gel (the amount of heat generating sources) and, simultaneously, the heat transfer capabilities of thermally conductive mixture increase (more graphite flakes with high thermal conductivity than PVP or silica gel). This makes it difficult to attribute increase of specific power from [5] or increase of thermal conductivity/diffusivity for both [5] and [22] to only graphite flakes addition.

In this study, the effect of expanded natural graphite as a thermally conductive additive on thermo-physical and uptake properties of several $CaCl_2$-based salt-in-porous-matrix composites is investigated. During synthesis, salt to silica gel and polyvinyl alcohol to silica gel ratios were fixed and the thermal additive (expanded natural graphite) to silica gel ratio was varied with care from 0 to 0.26 (0 to 20.5 wt.%, additive to silica gel ratio). This procedure allowed us to distinguish the effect of expanded natural graphite on the studied parameters from the effect of other composite components. The composites are characterized by a

transient plane source (thermal conductivity and thermal diffusivity), nitrogen adsorption porosimetry (specific surface area and total pore volume), and thermogravimetric sorption analysis (water sorption equilibrium) methods. A custom-built gravimetric large pressure jump (G-LPJ) testbed is used to evaluate the kinetics of water sorption (water uptake over time) for the selected samples. Sorption system performance parameters are calculated using equilibrium data and sorption kinetics and evaluated. The present results cover a range of composite compositions and coatings thicknesses. The early version of this research and preliminary results were presented at the IMPRES2022 conference, in Barcelona, Spain [25].

2. Materials and methods

2.1. Materials

Silica gel with an average pore diameter of 15 nm and particle sizes range of 250–500 μm (irregular grains; B150, SiliaFlash®; Silicycle, Inc., Quebec, Canada) was chosen as the host matrix of the sorption composite. Calcium chloride (anhydrous; Sigma-Aldrich) and polyvinyl alcohol (130,000 MW, 99%+ hydrolyzed; Amresco Inc.) were used as the impregnating salt and polymeric binder, respectively. Finally, expanded natural graphite (Timrex C-Therm 002; IMERYS Co., Quebec, Canada) was used as the thermally conductive additive in sorption composite samples.

2.2. Sorbent composite preparation

To study the effect of expanded natural graphite of $CaCl_2$-based salt-in-porous-matrix composites, eight different compositions were selected (Table 1). The sorption capacity of the salt in a mesoporous matrix is based on salt content (wt.%). Therefore, the greater salt content equals greater uptake. However, there is a limit on how much salt can be impregnated into the matrix under given sorption conditions before the salt solution starts to leak from the pores, which can be calculated based on the pore volume of the porous material [26]. In this study, based on the silica gel pore volume (Section 3.2, Table 2), calcium chloride ($CaCl_2$) density and sorption conditions, the salt-to-silica-gel ratio was calculated as ~0.43 (3/7). The binder-to-silica-gel ratio was also kept constant (~0.17 or 1/6) since this amount of polyvinyl alcohol (PVA130) was sufficient to bind grains together for all eight samples. Finally, the ratio between expanded natural graphite (ENG), used as the thermal conductive additive, and silica gel was changed from 0 to 0.26 (or 0 to 14 wt.% in the final composition).

The binder (PVA130) was dissolved in distilled water on a hotplate at 95 °C (1–2 hours). Dry calcium chloride was dissolved in the magnetically stirred solution (20 minutes). Expanded natural graphite (ENG) was added to the solution, sonicated for 10 minutes, and then magnetically stirred for 1 hour. Finally, dry silica gel grains were added to the solution and mixed for 30 minutes. The mixture was transferred to a flat dish and heated until the mixture thickened. For thermal conductivity/diffusivity measurement, three sets of two identical cylindrical samples with a diameter of 5 cm and thickness of 1 cm were prepared for each sample. For the sorption kinetic study, the mixture was moulded in a slab form with different thicknesses on a flat substrate made of a natural graphite sheet (NGS, 6.5 × 6.5 cm). All samples were oven-dried overnight with four temperature steps (80, 90, 100 and 130 °C). The dry masses of the consolidated samples were measured using an analytical balance (OHAUS AX124).

2.3. Characterization methods

The thermal conductivity and thermal diffusivity of the sorbent samples were determined using a transient plane source (TPS) "hot disk" thermal constants analyzer (TPS 2500S, ThermTest Inc., Fredericton, Canada) [27]. Two samples of the same composition were installed on top and bottom of the Hot Disk 5465 Kapton sensor (3.189 mm). The temperature rise in the sensor was then measured by analyzing the current and voltage, and this data was compared to the established resistivity of the nickel sensor. By examining the shape of the temperature-time graph, thermal conductivity and thermal diffusivity of the sample can be determined [27]. The tests were carried out at room temperature and relative humidity (T = 22 °C, RH = 30–35%). The measurements were repeated 5 times for each composition, and the results were averaged and presented here, with a confidence interval of 4.26% (for a 95% confidence level), to ensure repeatability.

The specific surface area (BET model [28]) and total specific pore volume of the pure B150 silica gel and chosen composite samples were measured using a nitrogen sorption analyzer (autosorb^{iQ}, Quantachrome Instruments, USA). For the drying process, composite samples were heated under a vacuum inside the analyzer for 12 hours at 120℃.

A thermogravimetric sorption analyzer (IGA-002, Hiden Isochema) was used to measure the water sorption isotherms of the composite samples. Sorption composites were placed in the device's sample basket, which was supported by a microbalance to measure the mass variations of the sorbent, while the pressure was regulated in the range of 0 - 3.6 kPa and step size of 0.2 kPa at 30 °C. More details about the thermogravimetric analyzer can be found elsewhere [22].

2.4. Gravimetric large pressure jump (G-LPJ) method

A custom-built gravimetric large pressure jump (G-LPJ) testbed was built and used to investigate the transient heat and mass transfer performance of the selected composite samples (Fig. 1). The G-LPJ testbed consisted of a vacuum chamber for the sample situated on the analytical balance (ME4002TE; Mettler Toledo), and evaporator (pool boiling shell-and-tube heat exchanger). The studied sample was placed on the cold plate (substrate) inside the vacuum chamber. Thermal interface material was added between them (thermal grease) to improve heat transfer and reduce thermal contact resistance between the sample and cold plate. The temperatures of the evaporator and the cold plate were controlled by separate heating/cooling circulators (Polystat 3C15; Cole-

Table 1
Composition of the prepared sorption composite samples and their thermal properties. $CaCl_2$/silica gel ratio of all samples was fixed at 3/7 (~0.43). PVA130/silica gel ratio was fixed at 1/6 (~0.17).

Sample codes	Sample composition				ENG/Silica gel ratio	Thermal conductivity, W/(m·K)	Thermal diffusivity, mm^2/s
	Silica gel, wt.%	Salt ($CaCl_2$), wt.%	Binder (PVA130), wt.%	Expanded Natural Graphite (ENG), wt.%			
SC	62.5	27	10.5	0	0	0.11	0.21
SCE1	62	26.5	10.5	1	0.02	0.15	0.29
SCE3	61	26	10	3	0.05	0.22	0.45
SCE4.5	60	25.5	10	4.5	0.08	0.27	0.60
SCE6	59	25.5	9.5	6	0.10	0.31	0.71
SCE8	58	25	9	8	0.14	0.37	0.87
SCE11	56	24	9	11	0.20	0.40	0.97
SCE14	54	23	9	14	0.26	0.41	1.03

Table 2
Composition, thicknesses and internal structure characteristics of the SC and SCE8 samples prepared for water sorption kinetics study.

Sample codes	Composite sample composition	Sample thickness (δ), mm	Sample mass, g	Specific surface area, m^2/g	Specific pore volume, cm^3/g	Average pore diameter, nm
S	Silica gel loose grains	–	–	289	1.05	13.8
SC-2	Silica gel + $CaCl_2$ + PVA130	2.3	5.2	134	0.50	14.8
SC-5		5.3	12.0			
SC-8		8.4	18.8			
SCE8–2	Silica gel + $CaCl_2$ + PVA130 +	2.4	4.7	109	0.42	15.4
SCE8–5	ENG	5.3	10.8			
SCE8–8		8.3	17.3			

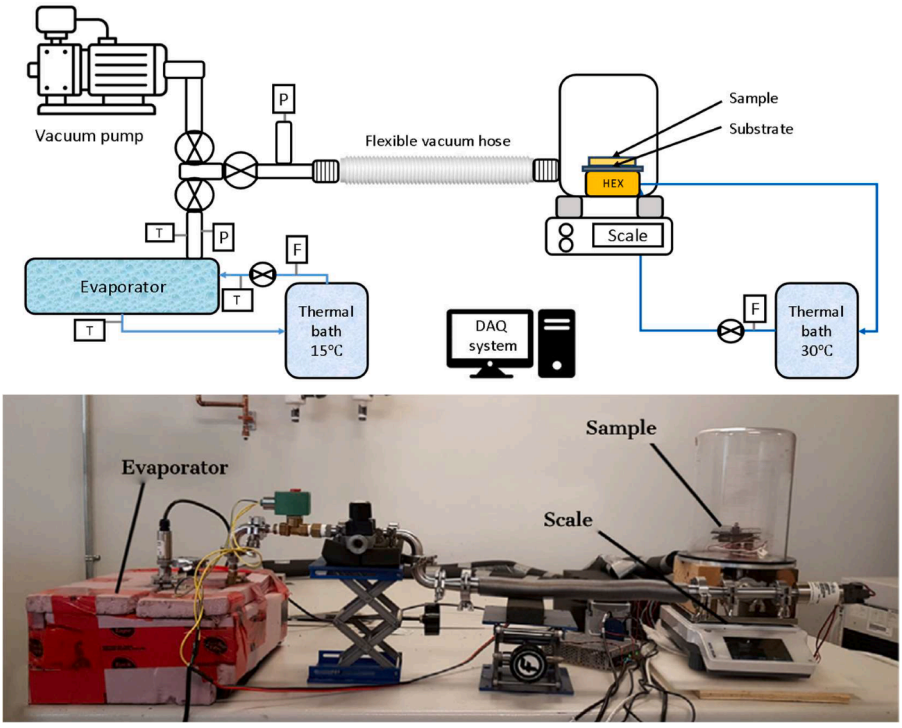

Fig. 1. Schematic diagram of custom-built gravimetric large pressure jump (G-LPJ) testbed test set-up. F – flow controllers, T – RTD temperature sensors, P – pressure sensors.

Parmer). Inlet and outlet temperatures of the heat transfer fluid side of the evaporator and vacuum chamber as well as the temperature of the gas inside the system were monitored by RTD temperature sensors (PT100 RTD Probe; Omega Sensing Solutions ULC). The flow rate of the heat transfer fluid was monitored by two ultrasonic flow meters (DUK-11N4HL343L; Kobold Messring GmbH). The pressure inside the system was monitored by two pressure sensors (PX309–005AI; Omega Sensing Solutions ULC). The evaporator was connected to the vacuum chamber by a flexible vacuum hose to allow the measurement of the sample's mass change. The evaporator and the vacuum chamber were separated by two ball valves. This configuration allows to evacuate the sample and set the vapor pressure in the evaporator simultaneously. To perform the test (pressure jump) both valves need to be open.

Before the experiment sorbent composite sample coated on the natural graphite sheet were completely dried in the oven at 120 °C. Then, sample was placed on the cold plate (HEX in Fig. 1) which was kept at a constant temperature of 30 °C. A very thin layer of thermal grease was applied between the natural graphite substrate and the cold plate to reduce thermal contact resistance. Before and during tests temperature of the gravimetric large pressure jump testbed, evaporator was maintained at 15 °C. The testbed's vacuum chamber was kept under vacuum for 0.5–1 hour before running the tests to ensure there was no moisture inside the sorbents, hoses, and the vacuum chamber. Finally, the valves between the chamber and the vacuum pump were shut and the valves between the evaporator and the chamber were opened to perform the water vapor pressure jump (from $p_0 = 0$ kPa to $p_{final} = 1.7$ kPa) which initiates the sorption process. The mass of the sample was monitored during the experiment to calculate the sorption kinetic curve and water uptake. All sensors and scale were connected to a data acquisition (DAQ) system to log the data and calculate the parameters.

3. Results and discussion

3.1. Thermal conductivity and thermal diffusivity

TPS measurements of thermal conductivity and thermal diffusivity on eight prepared samples showed that the thermal conductivity of the composites increases from 0.11 W/(m·K) for sample with no ENG to 0.37 W/(m·K) for sample with ENG/silica gel ratio of 0.14 (Fig. 2) linearly with the slope of 1.878 W/(m·K) and intercept of 0.116 W/(m·K). At higher ENG/silica gel ratios, thermal conductivity gradually increases up to 0.41 W/(m·K) (at ENG/silica gel ratio of 0.26) without following mentioned linear trend (Fig. 2).

The same trend is observed for thermal diffusivity (Fig. 2). It linearly increases from 0.21 mm^2/s (no ENG) to 0.87 mm^2/s (ENG/silica gel ratio is 0.14) and then gradually increases to 1.03 mm^2/s (ENG/silica gel

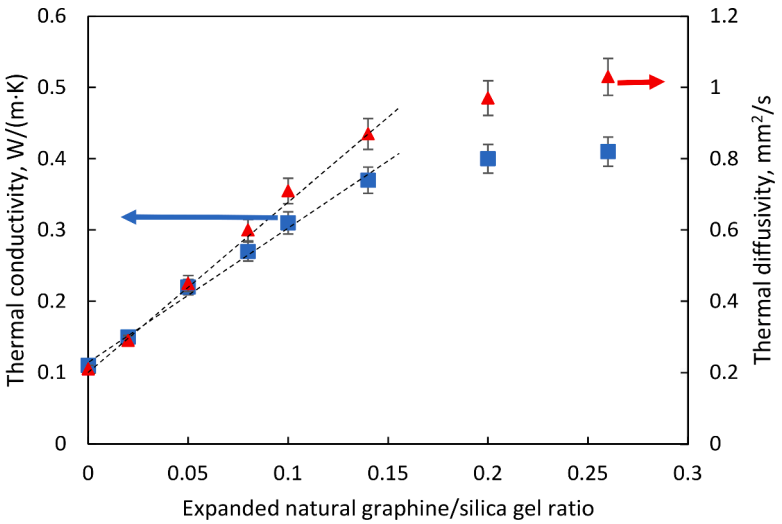

Fig. 2. Thermal conductivity (■) and thermal diffusivity (▲) of the silica gel composites with different expanded natural graphite/silica gel ratio, measured by transient plane source (TPS) "hot disc" method. Uncertainly of both measurements is 5%.

ratio is 0.26). For the linear trend, the slope is 4.845 mm^2/s and the intercept is 0.2067 mm^2/s.

A key heat conduction path in studied sorption composites is through the binder, which covers the silica gel particles and connects them. After adding conductive expanded natural graphite powder to the binder, these channels become more heat conductive compared to the ones with only PVA (Table 1). Fig. 3 shows the cross-section digital images of all the samples in Table 1. Particles in white colour show the salt-impregnated silica gels and black parts are expanded natural graphite and binder mixture. Microscope images of SC (Fig. 4a) and SCE8 (Fig. 4b) composites, taken by a Keyence VHX 5000 digital microscope showed a network made of PVA (SC) or PVA/ENG mixture (SCE8) that can act like a connected heat transfer pathway between the silica gel grains. This can explain the observed increase in thermal conductivity and thermal diffusivity between samples with and without expanded natural graphite added to the mixture.

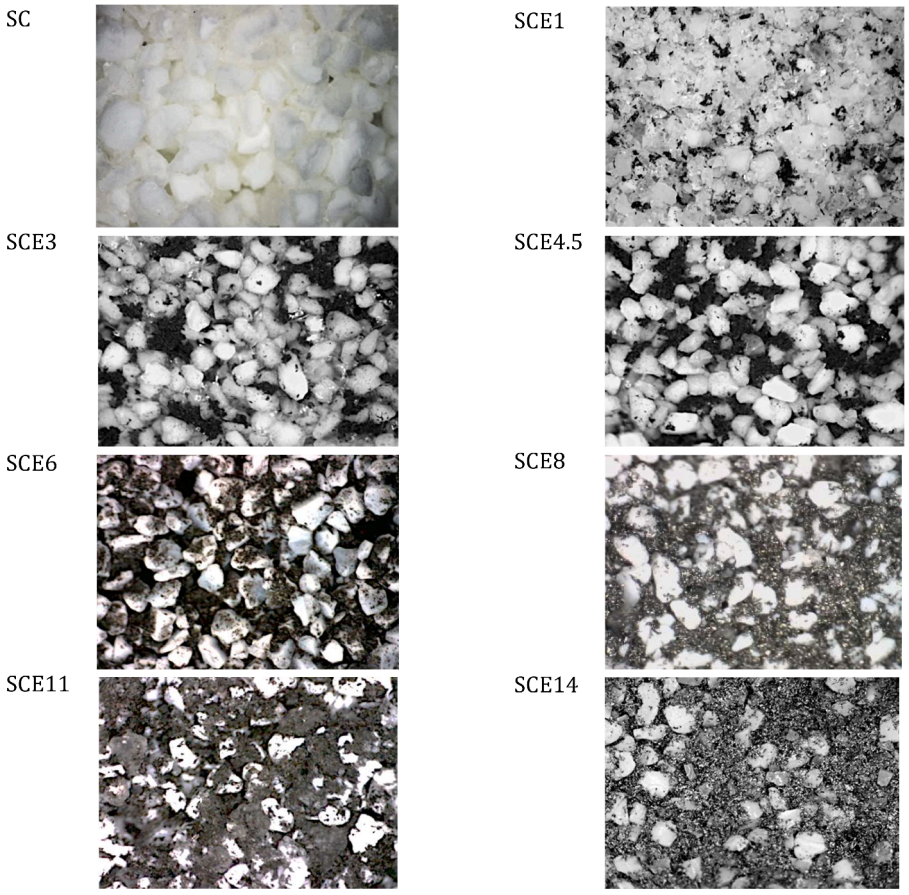

Fig. 3. Digital images from cross-section of samples with different ENG content taken by a DinoXcope digital microscope.

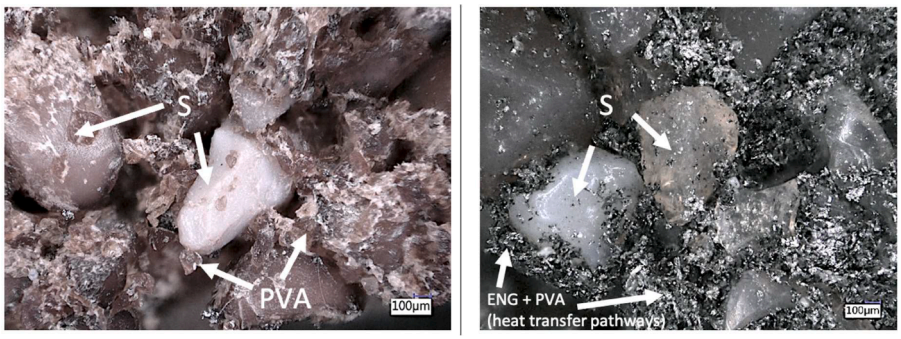

Fig. 4. Optical microscopic images of the SC (a), and SCE8 (b) samples, taken by a Keyence VHX 5000 digital microscope. Impregnated silica gel particles (S), expanded natural graphite (ENG), and polyvinyl alcohol binder (PVA) are shown by white arrows.

However, no thermal percolation [24] was observed contrary to the similar samples made with natural graphite flakes instead of ENG (Fig. 5a, [5]). This may be because ENG used in SCE samples has a smaller particle size (~81 μm) with lower density (~0.04 g/cm^3) compared to graphite flakes from [5] (mixture of 150 μm fine particles and 1.3 mm long flakes with a density about 1.9 g/cm^3). The smaller size and density of ENG particles allow them to more easily form heat transfer pathways required for thermal percolation which is observed already at 0.02 ENG/silica gel ratio. For the same effect to happen with graphite flakes composites, an additive-to-silica gel ratio of at least 0.25 is required (bigger, less numeral particles in the PVP/natural graphite mixture) [5]. A smaller increase of thermal conductivity and thermal diffusivity at ENG/silica gel ratios higher than 0.14 can indicate that most of the heat transfer pathways are already formed and the addition of more ENG only leads to an increase in their size ("reversed hockey stick").

By adding expanded natural graphite to the composition, the mass fraction of active materials (specifically, $CaCl_2$, Fig. 5b) in the composite and, consequently, water sorption capacity will linearly decrease with the increase of ENG/silica gel ratio. Thus, there is a trade-off between heat transfer improvement from ENG addition and sorption capacity. Moreover, because of the above-mentioned "reversed hockey stick" behaviour of the thermal properties of SCE composites, samples with high values of ENG/silica gel ratio may have worse kinetic performance due to lower sorption capacity. For example, SCE11 and SCE14 have higher thermal diffusivity (11.5% and 18.5%, respectively, compared to SCE8), but their water sorption capacity decreases by 4% and 8% respectively (Fig. 5a and b). At the same time, thermal diffusivity of SCE8 is 22.5% higher than that of SCE6 while water sorption capacity decreases only by 2% (Fig. 5a and b). Taking into account previous and that for the samples SCE11 and SCE14 thermal diffusivity increase with the increase of ENG content is lower than for SCE1–8 (which follow an observed linear trend, Fig. 2), the sample SCE8 (ENG/silica gel = 0.14) was considered having optimal composition and chosen for further characterization and kinetics study. The sample SC (without ENG) was also used to study the effect of ENG on water sorption kinetic and for comparison with SCE8.

3.2. Porosimetry measurement

The results of nitrogen porosimetry of silica gel B150 (S) and selected composites (SC and SCE8) are summarized in Table 2. Compared to pure silica gel particles, both specific surface area and total specific pore volume decrease for both composites. Considering SC (62.5 wt.% of silica gel, 27 wt.% of $CaCl_2$) and SCE8 (58 wt.% of silica gel, 25 wt.% of $CaCl_2$) composition (Table 1), measured pore volume of B150 $V_S = 1.05$ cm^3/g and density of dry $CaCl_2$ $\rho_{CaCl2} = 2.15$ g/cm^3, expected pore volume of SC is equal $V^e_{SC} = V_S \cdot 0.625 - 0.27/\rho_{CaCl2} = 0.53 \pm 0.05$ cm^3/g if all salt is inside pores of B150. Similarly, expected pore volume of SCE8 is equal $V^e_{SC8} = V_S \cdot 0.58 - 0.25/\rho_{CaCl2} = 0.37 \pm 0.04$ cm^3/g. A comparison of porosimetry data and these calculations show that in the case of the SC sample, all the salt is inside the grains of silica gel. In the case of SCE8, the measured pore volume is higher than calculated which may indicate that ENG (8 wt.% of composite) has some pores available for nitrogen even after mixing of thermal additive with PVA130.

The higher average pore diameter of SC and SCE8 compared to pure B150 indicates that salt is primarily accumulated in the smallest pores of the matrix during the preparation process (Table 2).

3.3. Sorption isotherms

Isotherm of water adsorption on silica gel B150 shows that silica gel

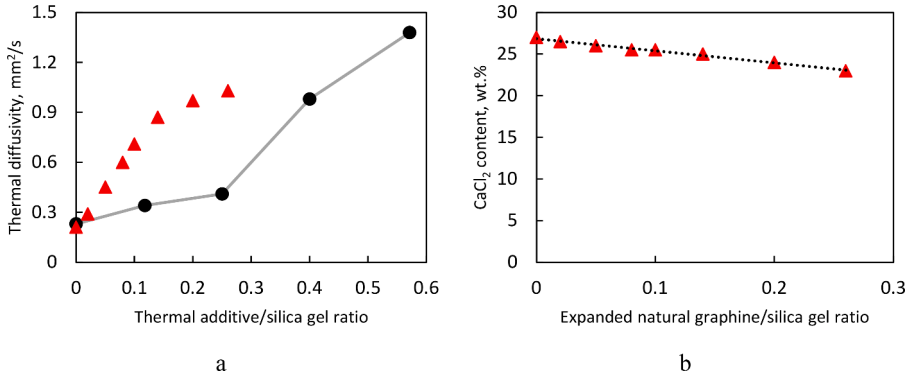

Fig. 5. a: thermal diffusivity of SC and SCE samples with ENG as the thermal additive (▲) and of $CaCl_2$/B150/PVP/graphite flakes samples (●, "hockey stick", [5]) depending on thermal additive/silica gel ratio. b: $CaCl_2$ content vs. ENG/silica gel ratio for SC and SCE samples.

itself cannot adsorb more than 0.1 $g_{water}/g_{sorbent}$ under the studied relative pressure range and temperature (p/p_0 = 0 - 0.85, 30 °C) since it is a mesoporous material with a relatively low surface area (Fig. 6, Table 2). However, after impregnating calcium chloride into the matrix, the sorption capacity of the composites increased significantly: w_{SC} = 0.67 g/g and w_{SCE8} = 0.64 g/g at p/p_0 = 0.8. The amount of water sorption for both studied composites was close to each other since the salt content is close as well (27 and 25 wt.%, respectively; Table 1). This and the similarity of the isotherms for SC and SCE8 show that ENG does not significantly affect the equilibrium between silica gel and calcium chloride.

3.4. Sorption performance evaluation

For the water sorption kinetics study, sorbent composites SC and SCE8 were prepared on natural graphite sheet substrate (Section 2.2) in three different thicknesses (Table 2): 2.3±0.1 mm (SC-2 and SCE8–2), 5.3±0.1 mm, (SC-5 and SCE8–5) and 8.3±0.1 mm (SC-8 and SCE8–8) - to evaluate the effect of ENG and sample thickness on the sorption kinetics.

It is worth mentioning that the reason for testing samples in this range of thicknesses was that, based on the literature [9,29,30], for the conventional sorption pairs and heat exchangers, when the sorbent thickness goes higher than this range, the heat and mass transfer resistance reduces the sorption performance drastically. On the other hand, very thin layers of the sorbent, reduce the active mass and capacity of the system. As an example, the optimum/tested thicknesses for these studies were between 2 mm to 8 mm.

The water uptake between completely dry condition (p/p_0 = 0) and final sorption sample conditions (p/p_0 = 0.4), which corresponds to the operating conditions T_{sorp} = 30 °C and T_{evap} = 15 °C, was calculated to be 0.34 ± 0.01 g/g and 0.33 ± 0.01 g/g for SC and SCE composite samples, respectively, according to the water sorption isotherms data (Section 3.3, Fig. 6). All six prepared samples were tested in the G-LPJ test set-up (Section 2.4, Figs. 7 and 8).

It was observed that for SC-2 water uptake reached the equilibrium value, established by thermo gravimetric test, after 25 minutes (Fig. 7). SC-5 and SC-9 reached equilibrium after 57 and 153 minutes, respectively (Fig. 7). For the SCE8 composites, a similar trend was observed: thicker samples took longer to reach equilibrium than thinner ones (Fig. 8). Water uptake reaches its equilibrium value after 15, 30, and 62 minutes for SCE8–2, SCE8–5, and SCE8–8, respectively. For both SC and SCE samples, the difference between sorption kinetics can be attributed to increase of samples' heat transfer resistances with thickness increase.

The difference between SC and SCE composites' kinetics of the same thickness can be explained by considering the addition of the expanded natural graphite. On one hand, the addition of the ENG increases thermal diffusivity of the sample which improves heat transfer. On the other hand, ENG, due to its low density decreases the density of the composite, which can be shown by their higher S/m = [heat transfer area]/[sorbent mass] values at constant thicknesses (Table 3). Lower density of the SCE means that it has more free volume for water vapor transfer between the grains which results in better external mass transfer.

Using kinetic data, two performance characteristics are calculated: specific cooling power (SCP) and specific surface cooling power (SSCP). SCP is defined as the ratio of evaporative cooling energy (Q_{evap}) to the product of cycle time (τ_{cycle}) and dry sorbent mass (m_{sorb}) (Eq. 2), was calculated based on the 70% equilibrium uptake (SCP-70%) or after 5 minutes (SCP-5 m) for both composite samples (Table 3).

$$SCP\ \left[\frac{W}{kg}\right] = \frac{Q_{evap}}{m_{sorb}\cdot\tau_{cycle}} = \frac{\Delta\omega\cdot h_{fg@T_{evap}}}{\tau_{cycle}}, \tag{2}$$

where the $h_{fg@T_{evap}}$ is the enthalpy of water evaporation at the evaporator temperature (at 15ºC) which is 2465.4 kJ/kg and $\Delta\omega$ is the net water uptake in gram water per gram of the composite at the 70% of equilibrium (SCP-70%) or after 5 minutes (SCP-5 m).

SSCP is defined as corresponding SCP multiplied by the mass of the studied composite m and divided by surface of the substrate S (Tables 2 and 3, Eq. 3):

$$SSCP\ \left[W/m^2\right] = \frac{SCP\cdot m}{S}, \tag{3}$$

The results showed that by increasing the sorbent thickness, specific cooling power decreased significantly. For example, by increasing the sorption composite thickness with expanded natural graphite from 2.4 to 8.3 mm, SCP-70% drops 4.2 times, from 1920 to 460 W/kg (Table 3). At the same time, by adding ENG to the composition it is possible to improve both SCP-70% and SCP-5 m (Table 3). For example, for a 5.3 ±0.1-mm thick samples, SCP-70% increased up to 77%: from 480 W/kg for SC-5 to 850 W/kg for SCE8–5. For the same samples, SCP-56

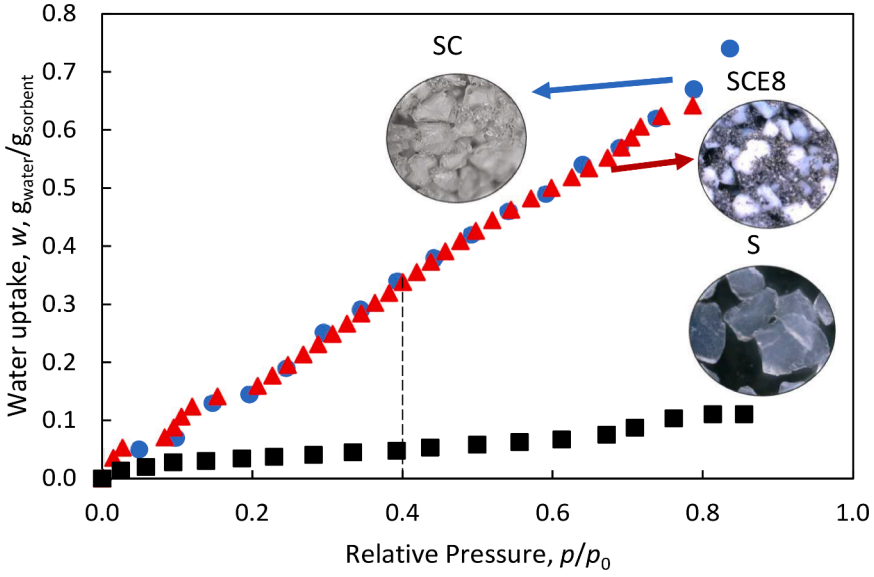

Fig. 6. Isotherms of water sorption by the loose grain silica gel B150 (S, ■) and composite sorbent materials (SC, ●, and SCE, ▲), measured by IGA-002 thermogravimetric sorption analyzer at 30 °C. Dash line – final sorption conditions for gravimetric large pressure jump (G-LPJ) tests. The uncertainty of the uptake measurements is 0.01 g/g.

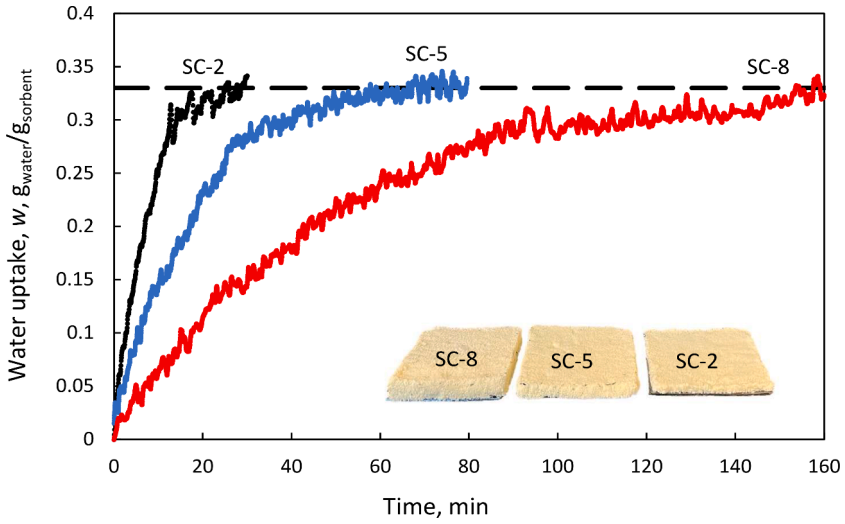

Fig. 7. Gravimetric large pressure jump (G-LPJ) water uptake kinetic curves for SC composite samples of different thicknesses. Dash line – maximal equilibrium water sorption uptake for the performed pressure jump (calculated using the water sorption isotherms data). The uncertainty analysis is in Appendix A.

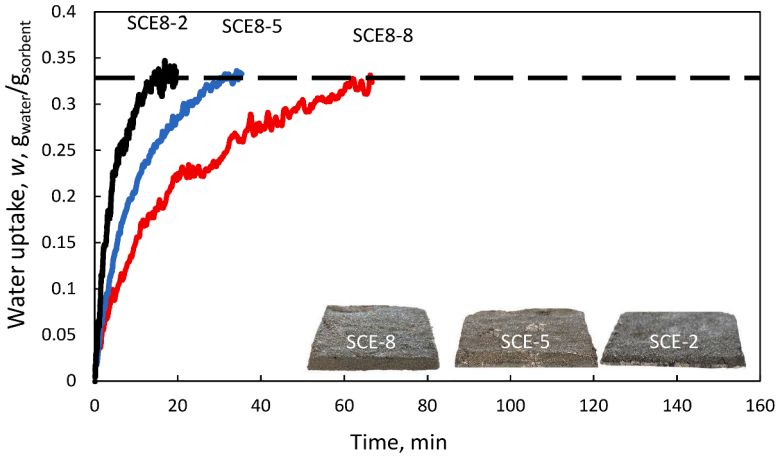

Fig. 8. Gravimetric large pressure jump (G-LPJ) water uptake kinetic curves for SCE8 composite samples with different thicknesses. Dash line – maximal equilibrium water sorption uptake for the performed pressure jump (calculated using the water sorption isotherms data). The uncertainty analysis is in Appendix A.

Table 3
Sorption performance parameters for studied composites.

Sample	Thickness, mm	SCP-70%, W/kg	SSCP-70%, W/m^2	SCP-5 m, W/kg	SSCP-5 m, W/m^2	*S/m*, cm^2/g
SC-2	2.3 ± 0.1	1070	1320	1355	1670	8.1
SC-5	5.3 ± 0.1	480	1360	760	2160	3.5
SC-8	8.4 ± 0.1	155	690	265	1180	2.2
SCE8–2	2.4 ± 0.1	1920	2140	1925	2140	8.9
SCE8–5	5.3 ± 0.1	850	2170	1180	3020	3.9
SCE8–8	8.3 ± 0.1	460	1880	780	3190	2.4

*SCP: specific cooling power in 70% of equilibrium uptake (SCP-70%) and after 5 minutes (SCP-5 min) for sorption (half-cycle); SSCP: specific surface cooling power calculated directly from SCP, mass of the corresponding sample and surface of the natural graphite sheet; *S/m*: substrate surface area to sorbent mass ratio.

increases by 55%: from 760 W/kg to 1180 W/kg.

Unexpectedly, specific power per surface area may increase with the sample's thickness increase. For longer cycles, SCP-70% finds its maximum in the case of samples SC-5 and SCE8–5 (Table 3). This can indicate that 5 mm samples can produce and transfer more heat through the sample's substrate while thicker samples become hindered by slower heat and mass transfer. However, for 5-minute cycle, SCE8–8 sample was found having highest SSCP (W/m^2). In its case SSCP-5 m = 3.19 kW/m^2 which is 6% higher than the SSCP-5 m for the sample SCE8–5 (3.02 kW/m^2). This result is different from what presented, for example, in ref. [31]; in that study, results show that both SCP and SSCP decrease with increasing thickness. However, in ref. [31] all the results obtained on LTJ setup where experiment is initiated by temperature jump. In our case, the process is initiated by the pressure jump (G-LPJ). Contrary to the temperature jump initiation usually present in sorption systems, in the case of pressure jump initiation the whole sample becomes exposed to the higher pressure of adsorptive which leads to faster initial sorption in the whole sample [32]. For this reason, the SGE8–8 sample with high thermal diffusivity and a bigger external surface than SGE8–5 has higher specific surface cooling power during the first 5 minutes of the process SSCP-5 m but a lower one at 70% water conversion SSCP-70%.

It is important to summarize that based on the test results, the samples of similar thicknesses with ENG have significantly higher SSCP than the samples without the additive (by 28%-170% for both SSCP-70% and SSCP-5 m, Table 3). This signifies that even though adding ENG decreases the overall capacity of the samples, their volumetric power is higher, which makes them better suited for sorption heat transformation (chiller) systems where both the volume of the sorbent material and its

power are important for designing the machine of the optimal size.

4. Conclusion

The effect of expanded natural graphite on thermo-physical properties and water sorption kinetics of the $CaCl_2$-based salt-in-porous-matrix composites with fixed salt/silica gel and binder/silica gel ratios was studied. The linear increase in thermal conductivity and thermal diffusivity with the increase of expanded natural graphite/silica gel ratio was discovered. It was attributed to the thermal percolation effect observed before for multi-component polymer blends similar to expanded natural graphite and polyvinyl alcohol mixture which is a part of the studied composites. It was found that by adding expanded natural graphite at a thermal additive/silica gel ratio of 0.14 to the calcium chloride/silica gel sorbent, thermal conductivity and thermal diffusivity would increase by 240% (0.11 W/(m·K) vs. 0.37 W/(m·K)) and 310% % (0.21 mm^2/s vs. 0.87 mm^2/s), respectively. This expanded natural graphite/silica gel ratio was found to be optimal for the studied combination of composite components because of the trade-off between the increase in thermal conductivity and thermal diffusivity of the samples and a decrease in water sorption capacity.

A custom-built gravimetric large pressure jump (G-LPJ) test bed was used to investigate the transient heat and mass transfer performance of the prepared sorption composites coated on a natural graphite sheet substrate. The sorption kinetic results showed that, for example, for a 5.3 ±0.1-mm thick sample, the specific cooling power increased up to 77% (from 480 W/kg to 850 W/kg), by adding expanded natural graphite at a thermal additive/silica gel ratio of 0.14. In addition to this, it was found that even though the specific cooling power decreases with the increase of sample thickness, the average cooling power per surface area can increase. Samples ranging from 2.4 to 5.3 mm in thickness are discovered to be ideal: specific surface cooling power at 70% water conversion can reach 2.17 kW/m^2 and 3.02 kW/m^2 during the first 5 minutes of the process for samples with expanded natural graphite.

Even though adding ENG to the samples decrease their sorption capacity per kg of composite, it leads to a significant increase of the specific surface cooling power (by 28%-170%) if compared to the samples without ENG of the same thickness. This means that by adding just a few percentages of ENG to the composition it is possible to increase cooling power per volume of the materials which makes such composites better suited for sorption heat transformation systems where not only power but the volume of the material is important.

CRediT authorship contribution statement

Salman Hassanabadi: Writing – review & editing, Writing – original draft, Validation, Methodology, Formal analysis, Data curation, Conceptualization. **Ilya S. Girnik:** Writing – review & editing, Investigation, Formal analysis. **Majid Bahrami:** Writing – review & editing, Supervision, Resources, Project administration, Funding acquisition, Conceptualization.

Declaration of competing interest

The authors declare that they have no known competing financial interests or personal relationships that could have appeared to influence the work reported in this paper.

Acknowledgement

This research was undertaken, in part, thanks to funding from the Canada Research Chairs Program, CRC-2018-00216. We acknowledge the support of the Natural Sciences and Engineering Research Council of Canada (NSERC), CREAT/554770-2021 and 2022-04371.

Appendix A. Uncertainty Analysis for G-LPJ test

The uncertainty in uptake calculation is obtained based on the method proposed by Moffat [33] as follows.

$$\omega = \frac{m_{sorptive}}{m_{sorbent}}$$

$$\frac{\delta\omega}{\omega} = \sqrt{\left(\frac{\delta m_{sorptive}}{\delta m_{sorptive}}\right)^2 + \left(\frac{\delta m_{sorbent}}{\delta m_{sorbent}}\right)^2} \cong \left(\frac{\delta m_{sorptive}}{\delta m_{sorptive}}\right)^2 = \frac{0.01\ g}{m_{sorptive}}$$

Sorbent mass was measured using an analytical balance (OHAUS AX124) with the accuracy of 0.0001 g, where the sorptive (water vapor) mass change was measured by precision balance (ML4002E, Mettler Toledo) with the accuracy of 0.01 g. Therefore, the sorbent mass uncertainty was negligible compared to that of sorptive.

According to the above calculations, for the water uptake values higher than 0.1 g/g, the uncertainty will be less than 10%.

Regarding the SCP, it should be calculated based on the uncertainty of the uptake (<10%), enthalpy of the evaporation (~0%), and cycle time (~0.33%), and it will be ~ 10%.

References

[1] Zhang, Y., Wang, R., May 2020. Sorption thermal energy storage: Concept, process, applications and perspectives. Energy Storage Mater. 27, 352–369. https://doi.org/10.1016/j.ensm.2020.02.024.
[2] Aristov, Y.I., 2020. Nanocomposite Sorbents For Multiple Applications. CRC Press.
[3] Wang, D., Zhang, J., Tian, X., Liu, D., Sumathy, K., 2014. Progress in silica gel–water adsorption refrigeration technology. Renew. Sustain. Energy Rev. 30, 85–104.
[4] Gordeeva, L., Aristov, Y.I., 2012. Composites 'salt inside porous matrix'for adsorption heat transformation: a current state-of-the-art and new trends. Int. J. Low-Carbon Technolog. 7 (4), 288–302.
[5] Bahrehmand, H., Khajehpour, M., Bahrami, M., 2018. Finding optimal conductive additive content to enhance the performance of coated sorption beds: an experimental study. Appl. Therm. Eng. 143, 308–315.
[6] Khajehpour, M., McCague, C., Shokoya, S., Bahrami, M., 2018. Effect of conductive additives on performance of CaCl2-silica gel sorbent materials. In: presented at the Heat Powered Cycles Conf, pp. 146–190.
[7] Helaly, H.O., Awad, M.M., El-Sharkawy, I.I., Hamed, A.M., Jan. 2019. Theoretical and experimental investigation of the performance of adsorption heat storage system. Appl. Therm. Eng. 147, 10–28. https://doi.org/10.1016/j.applthermaleng.2018.10.059.
[8] Darvish, MJ., Bahrehmand, H., Bahrami, M., Nov. 2021. An analytical design tool for pin fin sorber bed heat/mass exchanger. Int. J. Refriger. 131, 381–393. https://doi.org/10.1016/j.ijrefrig.2021.07.027.
[9] Bahrehmand, H., Bahrami, M., 2021. Optimized sorber bed heat and mass exchangers for sorption cooling systems. Appl. Therm. Eng. 185, 116348.
[10] Ashouri, M., Bahrami, M., Aug. 2022. Analytical solution for coupled heat and mass transfer in membrane-based absorbers. Int. J. Heat Mass Transf. 192, 122892 https://doi.org/10.1016/j.ijheatmasstransfer.2022.122892.
[11] Ashouri, M., Elsafi, A.M., Girnik, I.S., Bahrami, M., Aug. 2023. An analytical solution for heat and mass transfer in falling film absorption with arbitrary thermal boundary conditions. Appl. Therm. Eng. 231, 120891 https://doi.org/10.1016/j.applthermaleng.2023.120891.
[12] Mikhaeil, M., Gaderer, M., Dawoud, B., Sep. 2020. On the development of an innovative adsorber plate heat exchanger for adsorption heat transformation

processes; an experimental and numerical study. Energy 207, 118272. https://doi.org/10.1016/j.energy.2020.118272.
[13] Fumey, B., Weber, R., Baldini, L., Aug. 2017. Liquid sorption heat storage – a proof of concept based on lab measurements with a novel spiral fined heat and mass exchanger design. Appl. Energy 200, 215–225. https://doi.org/10.1016/j.apenergy.2017.05.056.
[14] Cortés, F.B., Chejne, F., Carrasco-Marín, F., Pérez-Cadenas, A.F., Moreno-Castilla, C., 2012. Water sorption on silica-and zeolite-supported hygroscopic salts for cooling system applications. Energy Convers. Manag. 53 (1), 219–223.
[15] Küsgens, P., et al., Apr. 2009. Characterization of metal-organic frameworks by water adsorption. Micropor. Mesopor. Mater. 120 (3), 325–330. https://doi.org/10.1016/j.micromeso.2008.11.020.
[16] Aristov, Y.I., 2007. New family of solid sorbents for adsorptive cooling: material scientist approach. J. Eng. Thermophys. 16 (2), 63–72.
[17] Aristov, Y.I., Gordeeva, L., 2009. 'Salt in a porous matrix' adsorbents: Design of the phase composition and sorption properties. Kinet. Cataly. 50 (1), 65–72.
[18] Gordeeva, L.G., Solovyeva, M.V., Sapienza, A., Aristov, Y.I., Apr. 2020. Potable water extraction from the atmosphere: Potential of MOFs. Renew. Energy 148, 72–80. https://doi.org/10.1016/j.renene.2019.12.003.
[19] Kakiuchi, H., et al., 2005. Water vapor adsorbent FAM-Z02 and its applicability to adsorption heat pump. Kagaku Kogaku Ronbunshu 31 (4), 273–277.
[20] Sharafian, A., Fayazmanesh, K., McCague, C., Bahrami, M., Dec. 2014. Thermal conductivity and contact resistance of mesoporous silica gel adsorbents bound with polyvinylpyrrolidone in contact with a metallic substrate for adsorption cooling system applications. Int. J. Heat Mass Transf. 79, 64–71. https://doi.org/10.1016/j.ijheatmasstransfer.2014.07.086.
[21] Gurgel, J., Filho, L.A., Grenier, P., Meunier, F., 2001. Thermal diffusivity and adsorption kinetics of silica-gel/water. Adsorption 7 (3), 211–219.
[22] Fayazmanesh, K., McCague, C., Bahrami, M., 2017. Consolidated adsorbent containing graphite flakes for heat-driven water sorption cooling systems. Appl. Therm. Eng. 123, 753–760.
[23] Huang, Y., Ellingford, C., Bowen, C., McNally, T., Wu, D., Wan, C., Apr. 2020. Tailoring the electrical and thermal conductivity of multi-component and multi-phase polymer composites. Int. Mater. Rev. 65 (3), 129–163. https://doi.org/10.1080/09506608.2019.1582180.
[24] Guo, Y., Ruan, K., Shi, X., Yang, X., Gu, J., Jun. 2020. Factors affecting thermal conductivities of the polymers and polymer composites: a review. Composit. Sci. Technol. 193, 108134 https://doi.org/10.1016/j.compscitech.2020.108134.
[25] Hassanabadi, S., Girnik, I., Bahrami, M., Oct. 2022. Kinetics of composite salt within porous matrix (CSPM) used in sorption systems. In: presented at the The Sixth International Symposium on Innovative Materials and Processes in Energy Systems. Barcelona, Spain.
[26] Girnik, I., McCague, C., Bahrami, M., 2023. "Salt in porous matrix" composites for sorption heat transformers: How to maximize sorption capacity and dynamic performance while avoiding leakage. In: presented at the Heat Powered Cycles.
[27] "ISO22007-2, 'Plastics-determination of thermal conductivity and thermal diffusivity-part 2: transient plane heat source (hot disc) method.' 2008.
[28] Brunauer, S., Emmett, P.H., Teller, E., Feb. 1938. Adsorption of gases in multimolecular layers. J. Am. Chem. Soc. 60 (2), 309–319. https://doi.org/10.1021/ja01269a023.
[29] Girnik, I.S., Grekova, A.D., Gordeeva, L.G., Aristov, Y.I., Oct. 2017. Dynamic optimization of adsorptive chillers: Compact layer vs. bed of loose grains. Appl. Therm. Eng. 125, 823–829. https://doi.org/10.1016/j.applthermaleng.2017.06.141.
[30] Santamaria, S., Sapienza, A., Frazzica, A., Freni, A., Girnik, I.S., Aristov, Y.I., 2014. Water adsorption dynamics on representative pieces of real adsorbers for adsorptive chillers. Appl. Energy 134, 11–19.
[31] Girnik, I.S., Aristov, Y.I., Jul. 2016. Dynamic optimization of adsorptive chillers: the 'AQSOA™-FAM-Z02 – water' working pair. Energy 106, 13–22. https://doi.org/10.1016/j.energy.2016.03.036.
[32] Girnik, I.S., Lombardo, W., Sapienza, A., Aristov, Y.I., Apr. 2022. Pressure- and temperature-initiated adsorption of water vapour in a finned flat-tube adsorber. Energy Convers. Manag. 258, 115487 https://doi.org/10.1016/j.enconman.2022.115487.
[33] Moffat, R.J., Jan. 1988. Describing the uncertainties in experimental results. Exper. Therm. Fluid Sci. 1 (1), 3–17. https://doi.org/10.1016/0894-1777(88)90043-X.